Journal of Inorganic Biochemistry 235 (2022) 111924

Contents lists available at ScienceDirect

Journal of Inorganic Biochemistry

journal homepage: www.elsevier.com/locate/jinorgbio

Chirality influence on the cytotoxic properties of anionic chiral bis (*N*-heterocyclic carbene)silver complexes

Carlos J. Carrasco [a], Francisco Montilla [a,*], Eleuterio Álvarez [b], José Manuel Calderón-Montaño [c], Miguel López-Lázaro [c], Agustín Galindo [a,*]

[a] Departamento de Química Inorgánica, Facultad de Química, Universidad de Sevilla, Aptdo 1203, 41071 Sevilla, Spain
[b] Instituto de Investigaciones Químicas, CSIC-Universidad de Sevilla, Avda. Américo Vespucio 49, 41092 Sevilla, Spain
[c] Departamento de Farmacología, Facultad de Farmacia, Universidad de Sevilla, Sevilla, Spain

ARTICLE INFO

Keywords:
NHC-dicarboxylate
Chiral
Silver
Anticancer
X-ray

ABSTRACT

Complexes $Na_3[Ag(NHC^R)_2]$, **2a-e** and **2b'-c'**, where NHC^R is a *N*-heterocyclic carbene of the 2,2′-(1*H*-2λ^3,3λ^4-imidazole-1,3-diyl)dicarboxylate type, were prepared by treatment of compounds HL^R, **1a-e** and **1b'-c'** (2-(1-(carboxy*alkyl*)-1H-imidazol-3-ium-3-yl)carboxylate), with silver oxide in the presence of aqueous sodium hydroxide. They were characterized by analytical, spectroscopic (infrared, IR, ^{1}H and ^{13}C nuclear magnetic resonance, NMR, and circular dichroism) and X-ray methods (**2a**). In the solid state, the anionic part of complex **2a**, $[Ag(NHC^H)_2]^{3-}$, shows a linear disposition of $C_{carbene}$-Ag-$C_{carbene}$ atoms and an eclipsed conformation of the two NHC ligands. The proposed bis(NHC) nature of the silver complexes was maintained in solution according to NMR and density functional theory (DFT) calculations. The cytotoxic activity of compounds **2** was evaluated against four cancer cell lines and one non-cancerous cell line and several structure-activity correlations were found for these complexes. For instance, the activity decreased when the bulkiness of the R alkyl group in $Na_3[Ag(NHC^R)_2]$ increased. More interesting is the detected chirality-anticancer relationship, where complexes $Na_3[Ag\{(S,S)\text{-}NHC^R\}_2]$ (R = Me, **2b**; ^{i}Pr, **2c**) showed better anticancer activity than those of their enantiomeric derivatives $Na_3[Ag\{(R,R)\text{-}NHC^R\}_2]$ (R = Me, **2b'**; ^{i}Pr, **2c'**).

1. Introduction

Transition metal complexes with *N*-Heterocyclic Carbene (NHC) scaffolds have become effective molecules that have gained enormous interest in recent decades due to the numerous applications they have demonstrated in several disciplines [1–4]. An area in which NHC ligands have shown great relevance, due to their robust coordination to metals, is their applications in medicinal chemistry. In particular, transition metal NHCs are the subject of a growing field of research as potential drugs against cancer disease [5–8]. For example, gold-NHC complexes have a well-recognized efficient anticancer activity [9,10], while studies on the anticancer effectiveness of Ag-NHC derivatives are in continuous progress [11–24]. In this area, the development of chiral and potentially water-soluble NHC ligands is of particular importance [25–27]. In fact, concerning chirality in organometallic anticancer complexes Romero and Sadler indicated years ago "*the comparative cytotoxicity between stereoisomers has hardly been explored*" [28]. From that statement to now, specific research about the anticancer-chirality relationship have been mainly focused in platinum derivatives [29–31] and, to our knowledge no related studies exist for chiral silver complexes.

Following our interest in the investigation of complexes containing amino acid-derived ligands [32–36] and their medicinal applications [37,38], we decided to explore the preparation of new silver complexes containing chiral NHC^R ligands, where NHC^R is a *N*-heterocyclic carbene of 2,2′-(1*H*-2λ^3,3λ^4-imidazole-1,3-diyl)dicarboxylate type (Scheme 1). Here, we present the synthesis and characterization of new water-soluble silver complexes $Na_3[Ag(NHC^R)_2]$ (R = H, **2a**), $Na_3[Ag\{(S,S)\text{-}NHC^R\}_2]$ (R = Me, **2b**; ^{i}Pr, **2c**; ^{i}Bu, **2d**; ^{s}Bu, **2e**) and $Na_3[Ag\{(R,R)\text{-}NHC^R\}_2]$ (R = Me, **2b'**; ^{i}Pr, **2c'**). The cytotoxic activity of these complexes versus four human cancer cell lines (melanoma cells MeWo, lung adenocarcinoma A549, bladder cancer cells T24, and gastric cancer cells KATO III) was evaluated and compared with a human non-malignant cell line (skin cells, HaCaT). The study of the cytotoxic activity of enantiomerically related complexes **2b**/**2b'** and **2c**/**2c'** is unprecedented for NHC-silver complexes and from the comparison of their activities a chiral-anticancer relationship was observed.

* Corresponding author.
E-mail address: galindo@us.es (A. Galindo).

https://doi.org/10.1016/j.jinorgbio.2022.111924
Received 30 May 2022; Received in revised form 20 June 2022; Accepted 4 July 2022
Available online 9 July 2022

2. Results and discussion

2.1. Synthesis and characterization of $Na_3[Ag(NHC^R)_2]$ (2a-e and 2b'-c') complexes

Initially, we planned the synthesis of bis(carbene) silver complexes **2** by reaction of compounds HL^R (**1**, 2-(1-(carboxy*alkyl*)-1H-imidazol-3-ium-3-yl)carboxylate) with Ag_2O in methanol. Surprisingly, dicarboxylate silver compounds, $[Ag(L^R)]$, were instead obtained, which were characterized as coordination polymeric species in the solid-state [37]. In solution, the C^2—H group of imidazolium in $[Ag(L^R)]$ complexes experienced a fast H—D exchange with D_2O, which was explained on the basis of the formation of a transient carbene intermediate according to DFT studies [37]. This prompted us to explore the reactivity of $[Ag(L^R)]$ with a base like aqueous sodium hydroxide in a NMR tube. The NMR spectrum of the crude reaction showed the disappearance of the C^2—H signals at *ca.* 8.9 (^{1}H) and 137 (^{13}C) ppm that suggests the formation of such a carbene species. In fact, the best synthetic procedure for the preparation of complexes **2** was by treating compounds HL^R, **1**, with Ag_2O in the presence of aqueous sodium hydroxide (Scheme 2). They were obtained as colorless crystals or solids in good yields, which were soluble in water or methanol but insoluble in organic solvents. Other source of silver(I) cations can be employed in the synthesis (silver nitrate or silver acetate), but silver oxide gave better results.

An intense and slightly broad band centered around 1600 cm^{-1} characterized the IR spectra of compounds **2** (Fig. S1, Supplementary data). This absorption was assigned to the antisymmetric COO vibrations of the carboxylate groups, while the symmetric COO vibrations appeared within the 1387–1371 cm^{-1} range. The ν_{as}(COO) band appeared at lower wavenumber than those of the parent compounds **1** (around 1625 cm^{-1}) and this fact suggests a major delocalization of the carboxylate group, in agreement with the observed solid-state structure (see below). ^{1}H and ^{13}C{^{1}H} NMR spectra of **2** (Figs. S2 and S3) displayed the expected signals of the corresponding alkyl groups and the typical pattern due to the imidazolium ring. For example, the equivalent CH groups at 4 and 5 ring positions give signals at *ca.* 7.5 and 120 ppm, in ^{1}H and ^{13}C{^{1}H} NMR, respectively. Carboxylate carbon atoms were identified in the ^{13}C{^{1}H} NMR spectra by singlets in the 170–175 ppm range, which are analogous to those recorded for related NHC-carboxylate silver complexes [38]. Although carbene ^{13}C resonances are often difficult to observe due to their long T_1 relaxation times or possible dynamic processes [39], ^{13}C{^{1}H} NMR spectra of complexes **2** showed the characteristic low field resonance for the C^2 atom. This signal appeared at around 180 ppm, but only for complexes **2c** and **2e** is well resolved showing the well-known pattern of two doublets due to coupling constants of $^1J_{CAg} = 185$ and 213 Hz. These values of $^1J_{CAg}$ are in agreement with an homoleptic binding mode of NHC ligands, C-Ag-C, in agreement with the proposed formulation, because larger coupling constants are often observed for heteroleptic binding modes, C-Ag-X or C-Ag-N [40,41]. Additionally, enantiomeric complexes $Na_3[Ag\{(S,S)\text{-}NHC^R\}_2]$ (R = Me, **2b**; ^{i}Pr, **2c**) and $Na_3[Ag\{(R,R)\text{-}NHC^R\}_2]$ (R = Me, **2b'**; ^{i}Pr, **2c'**) were spectroscopically characterized by circular dichroism (CD). Compounds **2b**/**2b'** showed a maximum at 271 nm, which obviously have different sign of θ_{obs}, while the maximum of **2c**/**2c'** appeared at 261 nm (see Fig. S4).

2.2. Structural characterization of complex 2a in the solid-state

Suitable crystals of complex $Na_3[Ag(NHC^H)_2]$, **2a**, were obtained by cooling to 0 °C a concentrated aqueous solution of **2a**. The anionic part of the complex, $[Ag(NHC^H)_2]^{3-}$, is shown in Fig. 1, while selected structural data are collected in Table S1. Anions are composed of the silver center and two bonded NHC^H ligands with Ag—C bond lengths of 2.077(7) Å. The typical linear arrangement of NHC^H groups was found with a $C_{carbene}$-Ag-$C_{carbene}$ angle of 173.1(3)°. They also display an eclipsed conformation of the two carbene ligands with a N1-C1-C1-N2 torsion angle of ca. 164°. These structural data agree well with those reported for silver mononuclear bis(carbene) complexes according to a CSD search (mean values of 2.088 Å and 177° for Ag—C and C-Ag-C, respectively, for 179 hits with R factor < 0.075 and restrictions 'no errors', 'non-disordered' and 'not polymeric') [42]. The C—O distances in the four carboxylate groups are similar (mean value of 1.249 Å). These carboxylate groups have two singular features, they are oriented to the same molecular side showing a C5-C4-C6-C7 torsion angle of *ca.* 0° and the angle between the planes defined by the COO atoms is only of *ca.* 19°. This arrangement allows the formation of a complex hydrogen bonding network with the hydrated sodium cations. These cations are placed in a zigzag arrangement along *a* axis with bridging water molecules of hydration that form discrete $[Na_5(H_2O)_{18}]^{5+}$ units (Fig. S5). These sodium units are maintained along this axis by forming hydrogen bonds with $[Ag(NHC^H)_2]^{3-}$ anions and two additional water molecules of hydration (Fig. 2). The resulting three-dimensional crystal packing is controlled by these hydrogen bonds, showing along *a* axis the approximately linear assemblage of sodium ions surrounded by the $[Ag(NHC^H)_2]^{3-}$ anions (Fig. S6). The structure of **2a** resembles to those found by Flores, de Jesús and coworkers in related bis(sulfonated NHC) silver compounds (refcodes SIFVEQ and SIFVOU) [43]. These complexes and **2a** are some of the few examples of anionic bis(NHC) silver complexes reported in the literature [44–47].

2.3. DFT analysis of complexes 2

The solid-state structure of complexes **2** was proposed to be analogous to that of **2a**, determined by X-ray diffraction methods. According to the NMR data, this structure is maintained in solution, resulting in complete dissociation of **2** in $[Ag(NHC^R)_2]^{3-}$ anions and solvated sodium cations. To further verify this hypothesis, DFT calculations for the anions **2a-e**, $[Ag\{(S,S)\text{-}NHC^R\}_2]^{3-}$, and **2b'-c'**, $[Ag\{(R,R)\text{-}NHC^R\}_2]^{3-}$, were performed at the B3LYP/LANL2DZ/6–311++G** level of theory. The resulting optimized structures of these complexes are shown in Fig. S7. The selected combination of the method and basis sets provides a good structural description of these complexes according to the satisfactory comparison of the calculated and experimental structural parameters of complex **2a**. In this case, the conformation of the NHC ligands in the optimized complex is not eclipsed but alternated with an angle between NHC planes of 88.2°. Different angles between these

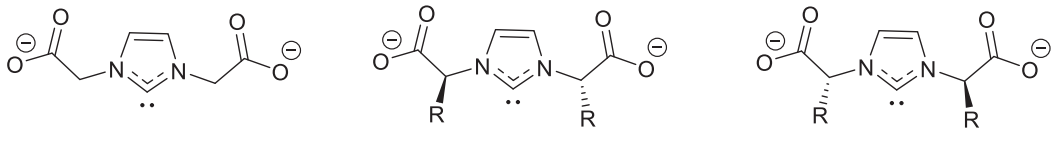

Scheme 1.

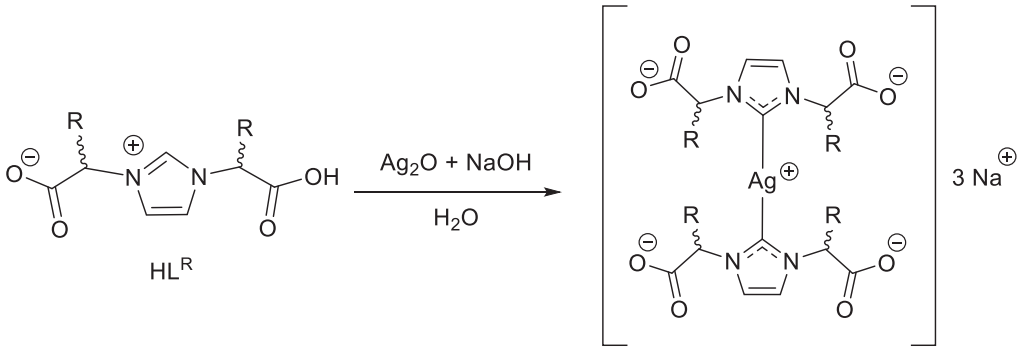

R = H, **1a**

(*S,S*)-HL^R

R = Me, **1b**; ^{i}Pr, **1c**; ^{i}Bu, **1d**; ^{s}Bu, **1e.**

(*R,R*)-HL^R

R = Me, **1b'**; ^{i}Pr, **1c'**

R = H, **2a**

(*S,S*)-

R = Me, **2b**; ^{i}Pr, **2c**; ^{i}Bu, **2d**; ^{s}Bu, **2e.**

(*R,R*)-

R = Me, **2b'**; ^{i}Pr, **2c'**

Scheme 2.

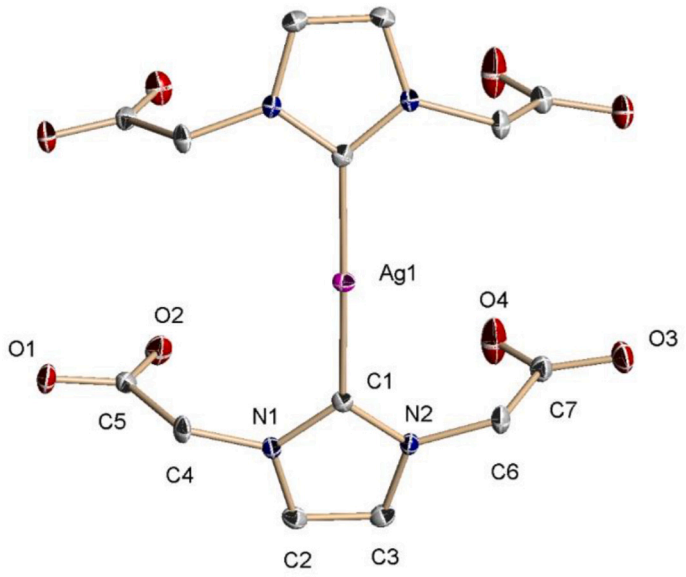

Fig. 1. Structure of the anionic part, $[Ag(NHC^H)_2]^{3-}$, of complex **2a**.

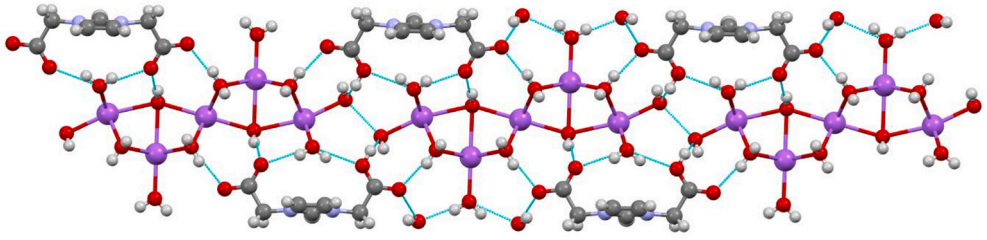

Fig. 2. Hydrogen bonding network between $[Ag(NHC^H)_2]^{3-}$ anions and sodium hydrated cations in complex **2a**.

planes were found for the other anions with staggered conformations (**2b**, 53.4°; **2c**, 48.4°; **2d**, 61.9°), except for **2e** where the angle is only 15.1°. The conformer of **2a** in which the carbene ligands are completely eclipsed is optimized as a transition state. This is destabilized by 7.0 kcal·mol^{-1} (ΔG) with respect to the staggered species and is characterized by one imaginary frequency with a very small absolute value.

This situation is completely similar to that first described by Frenking and coworkers in the theoretical analysis of bis(NHC) complexes of Group 11 metals [48]. The solid-state eclipsed conformation of NHC ligands can be explained on the basis of the extensive hydrogen bonding network between the carboxylate groups and the water hydration molecules of sodium cations, which counterbalances this energy difference. The ^{1}H and ^{13}C NMR chemical shifts were calculated for the optimized $[Ag(NHC^{R})_2]^{3-}$ anions of complexes **2a-c**. Excellent correlations between the calculated and experimental chemical shifts values were found (Fig. S8) confirming the formulation of these derivatives as bis (NHC) silver species and supporting their existence in solution.

2.4. Cytotoxic activity

The cytotoxicity of complexes **2** was evaluated in vitro by determining the half Inhibitory Concentrations (IC_{50}) against human BRAF wild-type melanoma MeWo cells, human lung adenocarcinoma A549, human bladder cancer cells T24, and human gastric cancer KATO III, as well as against human non-cancerous HaCaT cells. IC_{50} values were determined after 72 h of drug exposure to the cells using the resazurin assay. The results of viability are shown in Fig. 3 for enantiomeric complexes **2b**/**2b'** and **2c**/**2c'**, while for other **2** complexes are collected in Fig. S9. All results are also summarized in Table 1 and Table S2 (Selectivity Index values). Cisplatin and gemcitabine, two anticancer drugs used in clinics, were evaluated under the same experimental conditions (Fig. S9). Complexes **2** show cytotoxic activity against all

Table 1
IC_{50} values of compounds tested against human cell lines. After 72 h of treatment, cell viability was measured using the resazurin assay.[a]

Complex	IC_{50} (Mean ± SEM, μM)				
	HaCaT	A549	MeWo	T24	KATO III
2a	17.8 ± 0.2	33.0 ± 4.5	27.9 ± 7.0	17.6 ± 0.4	34.4 ± 8.7
2b	17.5 ± 0.3	33.8 ± 4.7	29.2 ± 5.6	18.3 ± 0.3	35.9 ± 9.4
2b'	19.1 ± 1.1	39.8 ± 4.2	33.6 ± 3.6	22.2 ± 3.3	38.3 ± 7.8
2c	18.4 ± 0.3	38.3 ± 3.8	31.6 ± 3.7	18.3 ± 0.1	35.2 ± 8.6
2c'	35.0 ± 5.8	48.0 ± 1.6	43.3 ± 3.4	48.2 ± 5.3	57.1 ± 3.0
2d	52.4 ± 1.5	69.9 ± 11.4	61.2 ± 15.6	52.6 ± 3.1	71.2 ± 8.7
2e	23.2 ± 4.1	44.2 ± 3.8	35.6 ± 4.1	36.7 ± 10.7	52.1 ± 1.7
Cisplatin	2.7 ± 0.2	2.7 ± 0.4	3.6 ± 0.5	1.6 ± 0.1	16.2 ± 0.9
Gemcitabine	0.0254 ± 0.0108	0.0038 ± 0.0004	0.0065 ± 0.0008	0.0027 ± 0.0005	0.0060 ± 0.0006

[a] Cell lines: HaCaT: Skin non-malignant; A549: Lung adenocarcinoma; MeWo: Melanoma BRAF WT; T24: Bladder cancer; KATO III: Gastric cancer. μM values are given as the mean value obtained from at least two independent experiments ± standard error of the mean (SEM) (see Experimental for details).

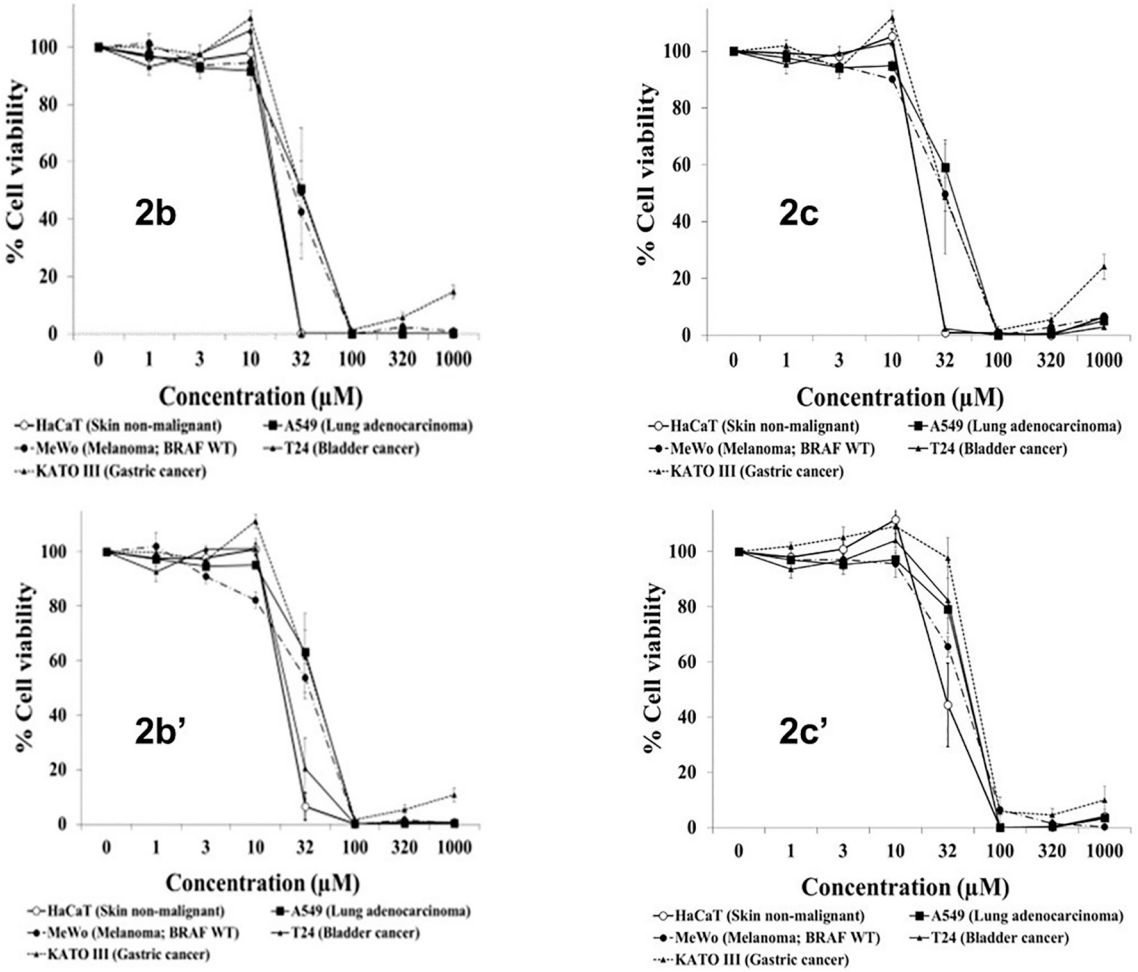

Fig. 3. Effect of complexes **2b**/**2b'** and **2c**/**2c'** on the viability of human non-malignant cells (HaCaT) and human cancer cells (A549, MeWo, T24 and KATO III). Cells were exposed to several concentrations of compounds for 72 h and cell viability was measured using the resazurin assay. Data represent mean ± SEM from at least two independent experiments.

cancer cell lines, within the range 17.6–71.2 μM, but all of them are less active than cisplatin and, by far, than gemcitabine (Table 1). Complexes **2** have activities that are in general slightly lower, or in some cases comparable, to those reported by Youngs et al. [19] and Tacke et al. [18] in several silver acetate NHCs, although with different cancerous cell lines. They described a better behavior against cancer cells of heteroleptic silver NHC compounds than those of homoleptic bis(NHC) derivatives. In fact, any of the IC_{50} values for our complexes **2** are higher than those reported for several silver chloride NHCs (for example, results of Roland [17] and Gautier [7] research groups). Given the anionic nature of **2**, we looked for an example of anionic bis(NHC) silver complex with a reported cytotoxic study to compare the cytotoxic activities of closely related compounds. Santini and coworkers published several complexes of this type [24,45], and they were evaluated for the same cell line, lung adenocarcinoma A549, which was also tested for **2**. Table S3 collects the IC_{50} values reported by Santini *et al.* and our data, which were ordered from the lowest to highest value. Complex $Na_4[AgCl(Im^{PrSO3})_2]$ [24] has the lowest value, 9.8 ± 2.3 μM, while complexes **2** with a mean IC_{50} value of 43.9 μM are between $Na_4[AgBr(Bzim')_2]$ and $Na_4[AgCl(Im')_2]$ derivatives (IC_{50} values of 25.0 and 53.1 μM, respectively [45]).

Concerning complexes **2**, the best activity was found versus Bladder cancer T24 cell line and the worst against gastric cancer KATO III. The analysis of IC_{50} values of **2a–e** and **2b'-c'** reveals a clear structure–anticancer effect relationship. The activity decreases when the steric properties of the R alkyl group in $Na_3[Ag(NHC^R)_2]$ complexes increase. In fact, complex $Na_3[Ag(NHC^H)_2]$, **2a**, displays the lowest IC_{50} value for each cell line. A similar relationship was recently described by us for related silver $\{Ag[NHC^{Mes,R}]\}_n$ complexes, where the antimicrobial activity versus Gram-negative bacteria *E. coli* and *P. aeruginosa* decreases when the bulkiness of the R alkyl group increases [38]. On the contrary, the inverse effect was described for NHC ruthenium complexes where the anticancer activity correlates with the complex lipophilicity [49]. A possible explanation of the reverse effect in **2** may be related with the presence of four hydrophilic carboxylate substituents in the two NHC ligands of the anions. An interesting result is the different anticancer behavior of enantiomerically related complexes **2b** / **2b'** and **2c** / **2c'**. Complexes **2b'** and **2c'** were prepared using the precursors **1b'** and **1c'** from the non-proteinaceous amino acids D-alanine and D-valine, respectively, while **2b** and **2c** derives from natural amino acids. Complex **2b** shows slightly better anticancer activity than that of their enantiomeric derivative **2b'**, but the activity of **2c** is clearly better than that of **2c'** for all tested cancer cell lines. These data suggest a chirality-anticancer correlation. An analogous tendency was recently observed by us in the antimicrobial study of amino acid based carboxylate silver complexes, where a slight different behavior was observed for enantiomerically related complexes [37].

Most available anticancer drugs usually do not cure the disease as a result of their limited selectivity toward cancer cells. They are toxic to both tumor and normal cells, especially normal cells with high proliferation rate, causing severe side effects such as skin ulcer, neurotoxicity, immunosuppression, etc. For this reason, the cytotoxic effect of complexes **2** was also evaluated against the human skin HaCaT cells, a non-cancerous cell line with a high proliferation rate. Complexes **2** showed IC_{50} values for human non-cancerous HaCaT cells (17.5 to 52.4 μM range) that are lower than those observed for cancerous cell lines (Fig. 3 and Table 1). However, it is worth mentioning that cisplatin was also more toxic to HaCaT cells than to most cancer cells tested. Therefore, the potential anticancer activity of **2** cannot be ruled out and more studies are needed to evaluate the selective anticancer activity of these complexes.

3. Experimental

3.1. General

All preparations and other operations were carried out under anaerobic conditions. Solvents were purified appropriately prior to use, using standard procedures. Cisplatin and Resazurin were purchased from Acros Organics and Sigma, respectively, while Gemcitabine was obtained from Pfizer. Other chemicals were obtained from several commercial sources and used as supplied. Zwitterionic imidazolium dicarboxylate compounds HL^R were prepared according to the literature procedures [50,33]. Infrared spectra were recorded using the ATR technique on Perkin-Elmer FT-IR Spectrum Two. NMR spectra were recorded at the *Centro de Investigaciones, Tecnología e Innovación* (CITIUS) of the University of Sevilla by using Avance III spectrometers. ^1H and $^{13}C\{^1H\}$ NMR shifts were referenced to residual signals from deuterated solvents. All data are reported in ppm downfield from Si $(CH_3)_4$. Electronic circular dichroism (CD) spectra were recorded in a Biologic Mos-450 spectropolarimeter (Barcelona, Spain). Elemental analyses (C, H, N) were conducted by the CITIUS of the University of Sevilla on an Elemental LECO CHNS 93 analyzer. High-resolution mass spectra were obtained on a QExactive Hybrid Quadrupole-Orbitrap mass spectrometer from Thermo Scientific (CITIUS of the University of Sevilla).

3.2. Cell lines

HaCaT cells (human keratinocytes [51]), A549 (human non-small cell lung cancer cells), KATO III (human gastric cancer cells), T24 (human bladder cancer cells), and MeWo (human BRAF wild-type melanoma cells) were purchased from Cell Lines Service (CLS). Cells were grown in Dulbecco's Modified Eagle's Medium (DMEM) that contained high glucose levels and L-glutamine. The medium was supplemented with 10% fetal bovine serum, 100 U/mL penicillin and 100 μg/mL streptomycin. All cells were maintained at 37 °C with 5% CO_2 in a humidified incubator.

3.3. Synthesis

3.3.1. Sodium bis(2,2′-(1H-2λ^3,3λ^4-imidazole-1,3-diyl)diacetate)argentate (I), $Na_3[Ag(NHC^H)_2]$ (2a)

Compounds HL^H, **1a**, (0.184 g, 1.00 mmol) and Ag_2O (0.058 g, 0.25 mmol) were mixed in a Schlenk flask and dissolved in deoxygenated H_2O (5 mL) under a nitrogen atmosphere. Then, NaOH (0.060 g, 1.5 mmol) was added and a dark brown solid was observed. The mixture was stirred for 16 h at room temperature in the dark. After that, the mixture was centrifuged, filtered and the filtrate was concentrated to a quarter of the volume using an intermediate trap and cooled to 0 °C. Uncolored crystals of compound **2a** were obtained (0.211 g, 73% yield). IR (ATR, cm^{-1}): 3167 (m), 3134 (m), 3108 (m), 2976 (w), 2941 (w), 1707 (w), 1610 (vs), 1563 (s), 1451 (m), 1419 (m), 1382 (vs), 1302 (vs), 1248 (m), 1137 (w), 1177 (m), 1109 (w), 1048 (w), 967 (w), 924 (w), 814 (m), 760 (m), 693 (s), 664 (s), 654 (vs), 579 (s), 470 (w), 422 (m). ^1H NMR (D_2O, 500 MHz): δ 4.71 (s, 8H, CH_2), 7.14 (s, 4H, CH, H^4/H^5), $^{13}C\{^1H\}$ NMR (D_2O, 125.78 MHz): δ 54.5 (s, CH_2), 122.5 (s, CH, C^4/C^5), 175.5 (s, COO), 181.9 (br s, C carbene). HR-MS (negative mode), found: m/z = 472.9866, calculated for $C_{14}H_{14}N_4O_8Ag$ ($[Ag(NHC^H)_2]^{3-}$ + 2H), 472.9868. Elemental Anal. Calc. for $C_{14}H_{16}N_4O_{10}AgNa_3$ (**2a**·$2H_2O$): C, 29.14; H, 2.79; N, 9.71. Found: C, 29.83; H, 2.83, N, 9.83%.

3.3.2. Sodium bis(2,2′-(1H-2λ^3,3λ^4-imidazole-1,3-diyl)dipropionate) argentate(I), $Na_3[Ag\{(S,S)\text{-}NHC^{Me}\}_2]$ (2b) and $Na_3[Ag\{(R,R)\text{-}NHC^{Me}\}_2]$ (2b')

Compounds (*S,S*)-HL^{Me}, **1b**, (0.212 g, 1.00 mmol), Ag_2O (0.058 g, 0.25 mmol) and NaOH (0.060 g, 1.5 mmol) were reacted following the same procedure described above. The resulting filtrate was concentrated

to dryness using an intermediate trap to afford compound **2b** as a white solid (0.309 g, 88% yield). IR (ATR, cm^{-1}): 3137 (w), 3096 (w), 2983 (w), 2940 (w), 2818 (w), 1733 (vw), 1587 (vs), 1455 (m), 1387 (s), 1356 (s), 1324 (m), 1298 (m), 1253 (m), 1169 (s), 1112 (w), 1079 (w), 1027 (m), 973 (w), 874 (m), 848 (w), 764 (w), 740 (w), 667 (m), 535 (w), 429 (w). ^{1}H NMR (CD_3OD, 500 Hz): δ 1.73 (d, $^3J_{HH}$ = 7 Hz, 12H, $CHCH_3$), 5.05 (c, $^3J_{HH}$ = 7 Hz, 4H, $CHCH_3$), 7.36 (s, 2H, CH, H^4/H^5). $^{13}C\{^1H\}$ NMR (CD_3OD, 75.47 MHz): δ 18.9 (s, $CHCH_3$), 60.5 (s, $CHCH_3$), 119.0 (s, CH, C^4/C^5), 176.2 (s, COO), 180.4 (br s, C carbene). HR-MS (negative mode), found: m/z = 529.0485, calculated for $C_{18}H_{22}N_4O_8Ag$ ($[Ag(NHC^{Me})_2]^{3-}$ + 2H), 529.0489. Elemental Anal. Calc. for $C_{18}H_{32}N_4O_{14}AgNa_3$ (**2b**·$6H_2O$): C, 30.65; H, 4.57; N, 7.94. Found: C, 30.89; H, 4.51; N, 7.23%. Following the same experimental method was prepared the complex $Na_3[Ag\{(R,R)\text{-}NHC^{Me}\}_2]$, **2b'**, (0.288 g, 94% yield). Compound **2b'** presented identical IR, ^{1}H and $^{13}C\{^1H\}$ NMR and HR-MS spectra that its enantiomer **2b**. Elemental Anal. Calc. for $C_{18}H_{22}N_4O_9AgNa_3$ (**2b'**·H_2O): C, 35.14; H, 3.60; N, 9.11. Found: C, 35.52; H, 4.28; N, 8.84%.

3.3.3. Sodium bis(2,2′-(1H-2λ^3,3λ^4-imidazole-1,3-diyl)bis(3-methylbutanoate))argentate(I), $Na_3[Ag\{(S,S)\text{-}NHC^{iPr}\}_2]$ (2c) and $Na_3[Ag\{(R,R)\text{-}NHC^{iPr}\}_2]$ (2c')

Compounds (*S*,*S*)-HL^{iPr}, **1c**, (0.268 g, 1.00 mmol), Ag_2O (0.058 g, 0.25 mmol) and NaOH (0.060 g, 1.5 mmol) were reacted following the same procedure described above. The resulting filtrate was concentrated to dryness using an intermediate trap to afford compound **2c** as a white solid (0.276 g, 72% yield). IR (ATR, cm^{-1}): 2960 (m), 2931 (m), 2873 (w), 1740 (vw), 1598 (vs), 1562 (m), 1466 (w), 1371 (vs), 1260 (m), 1240 (w), 1195 (w), 1166 (w), 1137 (w), 1105 (w), 1086 (w), 1041 (w), 980 (w), 950 (w), 918 (w), 870 (w), 841 (w), 825 (w), 749 (s), 638 (w), 603 (w), 503 (w), 439 (w). ^{1}H NMR (CD_3OD, 500 MHz): δ 0.85, 1.12 (d, $^3J_{HH}$ = 7.0 Hz, 12H, $CH(CH_3)_2$), 2.52 (o, $^3J_{HH}$ = 7.0 Hz, 4H, $CH(CH_3)_2$), 4.65 (d, $^3J_{HH}$ = 9 Hz, 4H, CH^iPr), 7.53 (s, 4H, CH, H^4/H^5). $^{13}C\{^1H\}$ NMR (CD_3OD, 125.78 MHz): δ 18.2, 19.2 (s, $CH(CH_3)_2$), 31.9 (s, $CH(CH_3)_2$), 74.5 (s, CH^iPr), 120.0 (s, CH, C^4/C^5), 174.9 (s, COO), 180.6 (dd, ^1J ($^{107}Ag—^{13}C$) = 185.3 Hz, ^1J ($^{109}Ag—^{13}C$) = 213.6 Hz, NCN). HR-MS (negative mode), found: m/z = 641.1732, calculated for $C_{26}H_{38}N_4O_8Ag$ ($[Ag(NHC^{iPr})_2]^{3-}$ + 2H), 641.1741. Elemental Anal. Calc. for $C_{26}H_{42}N_4O_{11}AgNa_3$ (**2c**·$3H_2O$): C, 40.90; H, 5.55; N, 7.34. Found: C, 40.37; H, 6.04; N, 7.17%. Following the same experimental method was prepared the complex $Na_3[Ag\{(R,R)\text{-}NHC^{iPr}\}_2]$, **2c'**, (0.330 g, 79% yield). Compound **2c'** presented identical IR, ^{1}H and $^{13}C\{^1H\}$ NMR and HR-MS spectra that its enantiomer **2c**. Elemental Anal. Calc. for $C_{26}H_{50}N_4O_{15}AgNa_3$ (**2c'**·$7H_2O$): C, 37.38; H, 6.03; N, 6.71. Found: C, 37.71; H, 6.23; N, 6.70%.

3.3.4. Sodium bis(2,2′-(1H-2λ^3,3λ^4-imidazole-1,3-diyl)bis(4-methylpentanoate))argentate(I), $Na_3[Ag\{(S,S)\text{-}NHC^{iBu}\}_2]$ (2d)

Compounds (*S*,*S*)-HL^{iBu} (**1d**) (0.299 g, 1.00 mmol), Ag_2O (0.058 g, 0.25 mmol) and NaOH (0.060 g, 1.5 mmol) were reacted following the same procedure described above. The resulting filtrate was concentrated to dryness using an intermediate trap to afford compound **2d** as a brown microcrystalline solid (0.320 g, 78% yield). IR (ATR, cm^{-1}): 3383 (vb), 3134 (m), 3095 (w), 2956 (m), 2928 (m), 2871 (m), 2154 (w), 1608 (vs), 1467 (m), 1382 (vs), 1368 (vs), 1289 (m), 1243 (w), 1224 (w), 1195 (w), 1169 (m), 1122 (w), 1047 (w), 1008 (w), 964 (w), 939 (w), 918 (w), 898 (w), 880 (w), 830 (w), 738 (m), 697 (m), 636 (w), 513 (w), 440 (w). ^{1}H NMR (CD_3OD, 500 MHz): δ 0.96, 0.99 (t, $^3J_{HH}$ = 7.0 Hz, 12H, $CH_2CH(CH_3)_2$), 1.42 (m, $^3J_{HH}$ = 7.0 Hz, 4H, $CH_2CH(CH_3)_2$), 2.06 (m, $^3J_{HH}$ = 7.0 Hz, 8H, $CH_2CH(CH_3)_2$), 4.86 (dd, $^3J_{HH}$ = 10.9 Hz, $^3J_{HH}$ = 5.6 Hz, 4H, CH^iBu), 7.64 (s, 4H, CH, H^4/H^5). $^{13}C\{^1H\}$ NMR (CD_3OD, 125.78 MHz): δ 20.2, 21.8 (s, $CH_2CH(CH_3)_2$), 24.8 (s, $CH_2CH(CH_3)_2$), 41.6 (s, $CH_2CH(CH_3)_2$), 63.9 (s, CH^iBu), 121.2 (s, CH, C^4/C^5), 172.9 (s, COO), 182.4 (br s, C carbene). HR-MS (negative mode), found: m/z = 697.2352, calculated for $C_{30}H_{46}N_4O_8Ag$ ($[Ag(NHC^{iBu})_2]^{3-}$ + 2H), 697.2372. Elemental Anal. Calc. for $C_{30}H_{50}N_4O_{11}AgNa_3$ (**2d**·$3H_2O$): C, 43.96; H, 6.15; N, 6.84. Found: C, 43.57; H, 6.28; N, 6.60%.

3.3.5. Sodium bis(2,2′-(1H-2λ^3,3λ^4-imidazole-1,3-diyl)bis(3-methylpentanoate))argentate(I), $Na_3[Ag\{(S,S)\text{-}NHC^{sBu}\}_2]$ (2e)

Compounds (*S*,*S*)-HL^{sBu}, **1e**, (0.299 g, 1.00 mmol), Ag_2O (0.058 g, 0.25 mmol) and NaOH (0.060 g, 1.5 mmol) were reacted following the same procedure described above. The resulting filtrate was concentrated to dryness using an intermediate trap to afford compound **2e** as a brown microcrystalline solid (0.355 g, 89% yield). IR (ATR, cm^{-1}): 3371 (w), 2963 (m), 2932 (m), 2877 (w), 1601 (vs), 1562 (m), 1453 (w), 1403 (s), 1373 (vs), 1258 (m), 1193 (w), 1156 (w), 1089 (w), 1050 (w), 976 (w), 915 (w), 880 (w), 851 (w), 835 (w), 742 (m), 642 (w), 616 (w), 558 (w), 428 (w). ^{1}H NMR (CD_3OD, 500 MHz): δ 0.85 (t, $^3J_{HH}$ = 7.0 Hz, 12H, CH_2CH_3), 1.03 (m, $^3J_{HH}$ = 7.0 Hz, 4H, CH_2CH_3), 1.05 (d, $^3J_{HH}$ = 7.0 Hz, 12H, $CHCH_3$), 1,25 (m, $^3J_{HH}$ = 7.0 Hz, 4H, CH_2CH_3), 2.24 (m, $^3J_{HH}$ = 7.0 Hz, 4H, $CHCH_3$), 4.67 (d, $^3J_{HH}$ = 10 Hz, 4H, CH^sBu), 7.49 (s, 4H, CH, H^4/H^5). $^{13}C\{^1H\}$ NMR (CD_3OD, 125.78 MHz): δ 10.4 (s, CH_2CH_3), 15.3 (s, $CHCH_3$), 25.0 (s, CH_2CH_3), 38.1 (s, $CHCH_3$), 73.4 (s, CH^sBu), 119.9 (s, CH, C^4/C^5), 174.9 (s, COO), 180.7 (dd, ^1J($^{107}Ag—^{13}C$) = 184.7 Hz, ^1J ($^{109}Ag—^{13}C$) = 213.2 Hz, NCN). HR-MS (negative mode), found: m/z = 697.2369, calculated for $C_{30}H_{46}N_4O_8Ag$ ($[Ag(NHC^{sBu})_2]^{3-}$ + 2H), 697.2372. Elemental Anal. Calc. for $C_{30}H_{48}N_4O_{10}AgNa_3$ (**2e**·$2H_2O$): C, 44.95; H, 6.04; N, 6.99. Found: C, 45.15; H, 6.32; N, 7.03%.

3.3.6. Cell viability assays

Exponentially growing cells (3000–6000 cells per well) were seeded in 96-well plates and allowed to grow for 24 h. Cells were then exposed to several concentrations of the new compounds or the anticancer drugs cisplatin and gemcitabine. After a 72-h treatment period, cell viability was estimated with the resazurin assay. This assay is a colorimetric technique based on the capability of viable cells to reduce the blue reagent resazurin to the pink soluble product resorufin. The amount of resorufin produced is generally proportional to the number of living cells. After the treatment period, cells were washed once with phosphate buffered saline (PBS), and 150 μL resazurin (20 μg/mL in medium) was added to each well. Because KATO III cells grow as a mixture of adherent and suspension cells, 50 μL resazurin (60 μg/mL in medium) was added directly without prior washing. The plates were incubated for 4–5 h at 37 °C, 5% CO2, and finally optical densities were measured at 540 and 620 nm with a multiwell plate spectrophotometer reader (Multiskan EX Labsystems). Cell viability was calculated as a percentage in relation to nontreated cells. Results were expressed as the means ± standard error of the mean (SEM). Data for complexes **2** are at least from four independent experiments. For statistical analysis, the *t*-test (paired, two-tailed) was used. A p value >0.05 is not considered statistically significant and is not represented by any symbol. A p value <0.05 is considered statistically significant and is indicated with an asterisk (*) and a p value <0.01 is indicated with a double asterisk (**). The statistical analysis was carried out to compare the cytotoxicity of a particular concentration of the compound between non-malignant HaCaT cells and a particular cancer cell line. The selectivity index (S.I.) values (Table S2) are useful in analyzing the selective anticancer activity of new compounds. S.I. values were calculated over each cancer cell line as the mean of the IC_{50} value in the non-cancerous cell line (HaCaT) by the IC_{50} in the respective cancer cell line obtained in each independent experiment.

3.3.7. Computational details

The electronic structure and geometries of the $[Ag(NHC^R)_2]^{3-}$ anions of **2a**-**e** were investigated by using density functional theory at the B3LYP level [52,53]. For the optimization the Ag atom was described with the LANL2DZ basis set [54], while 6–311++G(d,p) was used for the other atoms. Molecular geometries were optimized without symmetry restrictions. Frequency calculations were carried out at the same level of theory to identify the stationary points as minima (zero imaginary frequencies) and to provide the thermal correction to free energies at 298.15 K and 1 atm. The GIAO method was used for the NMR

calculations (^{1}H and ^{13}C NMR isotropic shielding tensors), which were carried out at the 6–311 + G(2d,p) level of theory. The DFT calculations were executed using the Gaussian 09 program package [55]. Coordinates of optimized compounds are collected in the Supplementary data (Table S4).

3.3.8. Single-crystal X-ray crystallography

A summary of the crystallographic data and the structure refinement results for compound **2a** is given in Table 2. Crystals of a suitable size for X-ray diffraction analysis were coated with dry perfluoropolyether and mounted on glass fibers and fixed in a cold nitrogen stream ($T = 193$ K) to the goniometer head. Data collection was carried out on a Bruker-AXS, D8 QUEST ECO, PHOTON II area detector diffractometer, using monochromatic radiation λ(Mo K$_\alpha$) = 0.71073 Å, by means of ω and φ scans with a width of 0.50°. The data were reduced (SAINT [56]) and corrected for absorption effects by the multi-scan method (SADABS) [57]. The structure was solved using direct methods (SIR-2002 [58]) and refined against all F^2 data by full-matrix least-squares techniques (SHELXTL-2018/3 [59]) minimizing $w[F_o^2\text{-}F_c^2]^2$. All non-hydrogen atoms were refined anisotropically. The hydrogen atoms were included from calculated positions and refined riding on their respective carbon atoms with isotropic displacement parameters. Since there are seven positive charges due to the metal cations (two silver and five sodium) and eight possible negative charges on the carboxylate anions, by symmetry in the crystal structure, a proton was added between the carboxylate groups for charge balance. A search for solvent accessible voids for this crystal structure using SQUEEZE [60] showed a small volume of potential solvent of 68 Å^3 for each (39 electron count), whose solvent content could not be identified or refined with the most severe restrictions, but due to the volume and the electrons present, it would coincide with four molecules of disordered water. The corresponding CIF data represent SQUEEZE treated structures with the solvent molecules handling as a diffuse contribution to the overall scattering, without specific atom position and excluded from the structural model. The SQUEEZE results were appended to the CIF. The corresponding crystallographic data were deposited with the Cambridge Crystallographic Data Centre as supplementary publications. CCDC 2169477 (**2a**) contain the supplementary crystallographic data for this paper. The data can be obtained free of charge via: https://www.ccdc.cam.ac.uk/structures/.

Table 2
Crystal data and structure refinement for compound **2a**.

Empirical formula	$C_{28}H_{69}Ag_2N_8Na_5O_{38}$
Formula weight	1456.60
Temperature	193(2) K
Wavelength	0.71073 Å
Crystal system	Monoclinic
Space group	$C_{2/m}$
a	15.9802(7) Å
b	15.4531(7) Å
c	12.8627(5) Å
α	90°
β	102.5720(10)°
γ	90°
Volume	3100.2(2) Å^3
Z	2
Density (calculated)	1.561 Mg/m^3
Absorption coefficient	0.765 mm^{-1}
F(000)	1492
Crystal size	0.500 × 0.300 × 0.200 mm^3
Theta range for data collection	2.270 to 25.248°
Index ranges	$-19 \le h \le 19$, $-18 \le k \le 18$, $-15 \le l \le 15$
Reflections collected	82,594
Independent reflections	2898 [R(int) = 0.0339]
Completeness to theta = 25.242°	98.8%
Absorption correction	Semi-empirical from equivalents
Max. and min. Transmission	0.7461 and 0.6241
Refinement method	Full-matrix least-squares on F^2
Data / restraints / parameters	2898 / 69 / 209
Goodness-of-fit on F^2	1.109
Final *R* indices [$I > 2\sigma(I)$]	$R_1 = 0.0813$, $wR_2 = 0.2215$
R indices (all data)	$R_1 = 0.0814$, $wR_2 = 0.2215$
Extinction coefficient	n/a
Largest diff. Peak and hole	4.857 and − 0.610 e·Å^{-3}

4. Conclusions

Complexes $Na_3[Ag(NHC^R)_2]$ (R = H, **2a**), $Na_3[Ag\{(S,S)\text{-}NHC^R\}_2]$ (R = Me, **2b**; ^{i}Pr, **2c**; ^{i}Bu, **2d**; ^{s}Bu, **2e**) and $Na_3[Ag\{(R,R)\text{-}NHC^R\}_2]$ (R = Me, **2b'**; ^{i}Pr, **2c'**) were obtained by reaction of the appropriate compound HL^R, **1**, (2-(1-(carboxy*alkyl*)-1H-imidazol-3-ium-3-yl)carboxylate) with Ag_2O in the presence of aqueous sodium hydroxide. They were spectroscopically characterized as anionic bis(NHC) silver complexes and, additionally, complex $Na_3[Ag(NHC^H)_2]$, **2a**, was structurally identified. The anion $[Ag(NHC^H)_2]^{3-}$ showed the expected linear arrangement of NHC^H groups and an eclipsed conformation of these carbene ligands. The cytotoxic behavior of these complexes was evaluated against five human cell lines: lung adenocarcinoma A549, Melanoma BRAF WT MeWo, Bladder cancer T24, gastric cancer KATO III and skin non-malignant HaCaT. Although the anticancer activity of **2** was lower than cisplatin and gemcitabine, two structure-activity correlations were found for these compounds. First, a decrease in the activity of the $Na_3[Ag(NHC^R)_2]$ species was observed when the bulkiness of the R alkyl group increased. Second, an interesting chirality-anticancer relationship was detected when comparing the activities of enantiomerically related complexes. Actually, complexes $Na_3[Ag\{(S,S)\text{-}NHC^R\}_2]$ (R = Me, **2b**; ^{i}Pr, **2c**) showed better cytotoxic activity than those of their enantiomeric derivatives $Na_3[Ag\{(R,R)\text{-}NHC^R\}_2]$ (R = Me, **2b'**; ^{i}Pr, **2c'**), which were synthesized with precursors **1b'** and **1c'** obtained from the non-proteinaceous amino acids D-alanine and D-valine, respectively. Although the IC_{50} values for non-cancerous cells HaCaT were lower than those observed for **2**, related behavior was observed for cisplatin in most cancer cells tested. For this reason, the potential anticancer activity of complexes **2** cannot be completely excluded and further studies are in progress to evaluate and improve the selective anticancer activity of these complexes.

Author contributions

Conceptualization, A. G. and F. M.; Synthesis and characterizations; C.J. C. and E. A.; Biological Studies: M. L.-L. and J.M. C.-M.; Investigation: C.J. C., F. M., E. A., J.M. C.-M., M. L.-L. and A. G.; resources: A. G., E. A. and M. L.-L.; writing—original draft preparation: A. G.; writing—review and editing: C.J. C., F. M., E. A., J.M. C.-M., M. L.-L. and A. G.; supervision: F- M., A. G. and M. L.-L.; project administration: A. G. and M. L.-L.; funding acquisition: A. G and M. L.-L.

Declaration of Competing Interest

The authors declare that they have no known competing financial interests or personal relationships that could have appeared to influence the work reported in this paper.

Data availability

Data will be made available on request.

Acknowledgements

Financial support from the Spanish Ministerio de Ciencia e Innovación (PGC2018-093443-B-I00) is gratefully acknowledged. C. J. C. thanks a research contract from PAIDI 2020, supported by the European Social Fund and the Junta de Andalucía. This research was partially funded by the University of Sevilla through the "VI Plan Propio de Investigación y Transferencia" (grant number VIPPIT-2021-I.5). The authors thank to *Centro de Investigaciones, Tecnología e Innovación*

(CITIUS) of the University of Sevilla for providing several research services and to *Centro de Servicios de Informática y Redes de Comunicaciones* (CSIRC), Universidad de Granada, for providing the computing time. The authors thank Dr. José A. Lebrón for recording the CD spectra.

Appendix A. Supplementary data

Supplementary data to this article can be found online at https://doi.org/10.1016/j.jinorgbio.2022.111924.

References

[1] P. Bellotti, M. Koy, M.N. Hopkinson, F. Glorius, Recent advances in the chemistry and applications of N-heterocyclic carbenes, Nat. Rev. Chem. 5 (2021) 711–725, https://doi.org/10.1038/s41570-021-00321-1.
[2] V.A. Voloshkin, N.V. Tzouras, S.P. Nolan, Recent advances in the synthesis and derivatization of N-heterocyclic carbene metal complexes, Dalton Trans. 50 (2021) 12058–12068, https://doi.org/10.1039/d1dt01847g.
[3] Y. Wang, J.-P. Chang, R. Xu, S. Bai, D. Wang, G.-P. Yang, L.-Y. Sun, P. Li, Y.-F. Han, N-heterocyclic carbenes and their precursors in functionalised porous materials, Chem. Soc. Rev. 50 (2021) 13559–13586, https://doi.org/10.1039/d1cs00296a.
[4] A. Ferry, K. Schaepe, P. Tegeder, C. Richter, K.M. Chepiga, B.J. Ravoo, F. Glorius, Negatively charged N-heterocyclic carbene-stabilized Pd and au nanoparticles and efficient catalysis in water, ACS Catal. 5 (2015) 5414–5420, https://doi.org/10.1021/acscatal.5b01160.
[5] A. Gautier, F. Cisnetti, Advances in metal-carbene complexes as potent anti-cancer agents, Metallomics 4 (2012) 23–32, https://doi.org/10.1039/c1mt00123j.
[6] L. Mercs, M. Albrecht, Beyond catalysis: N-heterocyclic carbene complexes as components for medicinal, luminescent, and functional materials applications, Chem. Soc. Rev. 39 (2010) 1903–1912, https://doi.org/10.1039/b902238b.
[7] M.L. Teyssot, A.S. Jarrousse, M. Manin, A. Chevry, S. Roche, F. Norre, C. Beaudoin, L. Morel, D. Boyer, R. Mahiou, A. Gautier, Metal-NHC complexes: a survey of anti-cancer properties, Dalton Trans. (2009) 6894–6902, https://doi.org/10.1039/b906308k.
[8] W. Liu, R. Gust, Update on metal N-heterocyclic carbene complexes as potential anti-tumor metallodrugs, Coord. Chem. Rev. 329 (2016) 191–213, https://doi.org/10.1016/j.ccr.2016.09.004.
[9] M. Mora, M.C. Gimeno, R. Visbal, Recent advances in gold-NHC complexes with biological properties, Chem. Soc. Rev. 48 (2019) 447–462, https://doi.org/10.1039/c8cs00570b.
[10] N. Estrada-Ortiz, F. Guarra, I.A.M. de Graaf, L. Marchetti, M.H. de Jager, G.M. M. Groothuis, C. Gabbiani, A. Casini, Anticancer gold N-heterocyclic carbene complexes: a comparative in vitro and ex vivo study, ChemMedChem. 12 (2017) 1429–1435, https://doi.org/10.1002/cmdc.201700316.
[11] N. Şahin, S. Şahin-Bölükbaşı, H. Marşan, Synthesis and antitumor activity of new silver(I)-N-heterocyclic carbene complexes, J. Coord. Chem. 72 (2019) 3602–3613, https://doi.org/10.1080/00958972.2019.1697808.
[12] J.C. Garrison, W.J. Youngs, Ag(I) N-heterocyclic carbene complexes: synthesis, structure, and application, Chem. Rev. 105 (2005) 3978–4008, https://doi.org/10.1021/cr050004s.
[13] J.C.Y. Lin, R.T.W. Huang, C.S. Lee, A. Bhattacharyya, W.S. Hwang, I.J.B. Lin, Coinage metal-N-heterocyclic carbene complexes, Chem. Rev. 109 (2009) 3561–3598, https://doi.org/10.1021/cr8005153.
[14] S. Kankala, N. Thota, F. Björkling, M.K. Taylor, R. Vadde, R. Balusu, Silver carbene complexes: an emerging class of anticancer agents, Drug Dev. Res. 80 (2019) 188–199, https://doi.org/10.1002/ddr.21478.
[15] N.A. Johnson, M.R. Southerland, W.J. Youngs, Recent developments in the medicinal applications of silver-NHC complexes and imidazolium salts, Molecules 22 (2017) 1263, https://doi.org/10.3390/molecules22081263.
[16] C.H. Wang, W.C. Shih, H.C. Chang, Y.Y. Kuo, W.C. Hung, T.G. Ong, W.S. Li, Preparation and characterization of amino-linked heterocyclic carbene palladium, gold, and silver complexes and their use as anticancer agents that act by triggering apoptotic cell death, J. Med. Chem. 54 (2011) 5245–5249, https://doi.org/10.1021/jm101096x.
[17] S. Roland, C. Jolivalt, T. Cresteil, L. Eloy, P. Bouhours, A. Hequet, V. Mansuy, C. Vanucci, J.-M. Paris, Investigation of a series of silver-N-heterocyclic carbenes as antibacterial agents: activity, synergistic effects, and cytotoxicity, Chem. - A Eur. J. 17 (2011) 1442–1446, https://doi.org/10.1002/chem.201002812.
[18] S. Patil, J. Claffey, A. Deally, M. Hogan, B. Gleeson, L.M.M. Méndez, H. Müller-Bunz, F. Paradisi, M. Tacke, Synthesis, cytotoxicity and antibacterial studies of p-methoxybenzyl- substituted and benzyl-substituted N-heterocyclic carbene-silver complexes, Eur. J. Inorg. Chem. 2010 (2010) 1020–1031, https://doi.org/10.1002/ejic.200900889.
[19] T.J. Siciliano, M.C. Deblock, K.M. Hindi, S. Durmus, M.J. Panzner, C.A. Tessier, W. J. Youngs, Synthesis and anticancer properties of gold(I) and silver(I) N-heterocyclic carbene complexes, J. Organomet. Chem. 696 (2011) 1066–1071, https://doi.org/10.1016/j.jorganchem.2010.10.054.
[20] K.M. Hindi, T.J. Siciliano, S. Durmus, M.J. Panzner, D.A. Medvetz, D.V. Reddy, L. A. Hogue, C.E. Hovis, J.K. Hilliard, R.J. Mallet, C.A. Tessier, C.L. Cannon, W. J. Youngs, Synthesis, stability, and antimicrobial studies of electronically tuned silver acetate N -heterocyclic carbenes, J. Med. Chem. 51 (2008) 1577–1583, https://doi.org/10.1021/jm0708679.
[21] D.A. Medvetz, K.M. Hindi, M.J. Panzner, A.J. Ditto, Y.H. Yun, W.J. Youngs, Anticancer activity of ag(I) N-heterocyclic carbene complexes derived from 4,5-dichloro-1H-imidazole, Metal-Based Drugs 2008 (2008) 1–7, https://doi.org/10.1155/2008/384010.
[22] F. Guarra, N. Busto, A. Guerri, L. Marchetti, T. Marzo, B. García, T. Biver, C. Gabbiani, Cytotoxic Ag(I) and Au(I) NHC-carbenes bind DNA and show TrxR inhibition, J. Inorg. Biochem. 205 (2020), 110998, https://doi.org/10.1016/j.jinorgbio.2020.110998.
[23] S.J. Allison, M. Sadiq, E. Baronou, P.A. Cooper, C. Dunnill, N.T. Georgopoulos, A. Latif, S. Shepherd, S.D. Shnyder, I.J. Stratford, R.T. Wheelhouse, C.E. Willans, R. M. Phillips, Preclinical anti-cancer activity and multiple mechanisms of action of a cationic silver complex bearing N-heterocyclic carbene ligands, Cancer Lett. 403 (2017) 98–107, https://doi.org/10.1016/j.canlet.2017.04.041.
[24] V. Gandin, M. Pellei, M. Marinelli, C. Marzano, A. Dolmella, M. Giorgetti, C. Santini, Synthesis and in vitro antitumor activity of water soluble sulfonate- and ester-functionalized silver(I) N-heterocyclic carbene complexes, J. Inorg. Biochem. 129 (2013) 135–144, https://doi.org/10.1016/j.jinorgbio.2013.09.011.
[25] D. Janssen-Müller, C. Schlepphorst, F. Glorius, Privileged chiral N-heterocyclic carbene ligands for asymmetric transition-metal catalysis, Chem. Soc. Rev. 46 (2017) 4845–4854, https://doi.org/10.1039/c7cs00200a.
[26] H. Diaz Velazquez, F. Verpoort, N-heterocyclic carbene transition metal complexes for catalysis in aqueous media, Chem. Soc. Rev. 41 (2012) 7032–7060, https://doi.org/10.1039/c2cs35102a.
[27] L.A. Schaper, S.J. Hock, W.A. Herrmann, F.E. Kühn, Synthesis and application of water-soluble NHC transition-metal complexes, Angew. Chem. Int. Ed. 52 (2013) 270–289, https://doi.org/10.1002/anie.201205119.
[28] M.J. Romero, P.J. Sadler, Chirality in organometallic anticancer complexes, in: Bioorganometallic Chemistry, John Wiley & Sons, Ltd, 2015, pp. 85–116, https://doi.org/10.1002/9783527673438.ch03.
[29] F. Arnesano, A. Pannunzio, M. Coluccia, G. Natile, Effect of chirality in platinum drugs, Coord. Chem. Rev. 284 (2015) 286–297, https://doi.org/10.1016/j.ccr.2014.07.016.
[30] M. Benedetti, J. Malina, J. Kasparkova, V. Brabec, G. Natile, Chiral discrimination in platinum anticancer drugs, Environ. Health Perspect. 110 (2002) 779–782, https://doi.org/10.1289/ehp.02110s5779.
[31] P. Papadia, A. Barbanente, N. Ditaranto, J.D. Hoeschele, G. Natile, C. Marzano, V. Gandin, N. Margiotta, Effect of chirality on the anticancer activity of Pt(II) and Pt(IV) complexes containing 1R,2R and 1S,2S enantiomers of thetrans-1,2-diamino-4-cyclohexene ligand (DACHEX), an analogue of diaminocyclohexane used in oxaliplatin, Dalton Trans. 50 (2021) 15655–15668, https://doi.org/10.1039/d1dt02255e.
[32] P. Caballero, R.M.P. Colodrero, Del M. Conejo, A. Pastor, E. Álvarez, F. Montilla, C. J. Carrasco, A.I. Nicasio, A. Galindo, Homochiral imidazolium-based dicarboxylate compounds: structure and solution behaviour, Inorganica Chim. Acta 513 (2020), 119923, https://doi.org/10.1016/j.ica.2020.119923.
[33] C. Carrasco, F. Montilla, A. Galindo, Molybdenum-catalyzed enantioselective sulfoxidation controlled by a nonclassical hydrogen bond between coordinated chiral imidazolium-based dicarboxylate and peroxido ligands, Molecules 23 (2018) 1595, https://doi.org/10.3390/molecules23071595.
[34] A.I. Nicasio, F. Montilla, E. Álvarez, R.P. Colodrero, A. Galindo, Synthesis and structural characterization of homochiral 2D coordination polymers of zinc and copper with conformationally flexible ditopic imidazolium-based dicarboxylate ligands, Dalton Trans. 46 (2017) 471–482, https://doi.org/10.1039/c6dt03712g.
[35] E. Borrego-Blanco, A.I. Nicasio, E. Alvarez González, F. Montilla, J.M. Córdoba, A. Galindo, Synthesis and structural characterization of homochiral coordination polymers with imidazole-based monocarboxylate ligands, Dalton Trans. 48 (2019) 8731–8739, https://doi.org/10.1039/c9dt01237k.
[36] A. Sánchez, J. Sanz-Garrido, C.J. Carrasco, F. Montilla, E. Álvarez, C. González-Arellano, J. Carlos Flores, A. Galindo, Synthesis and characterization of chiral bidentate bis(N-heterocyclic carbene)-carboxylate palladium and nickel complexes, Inorg. Chim. Acta 537 (2022), 120946, https://doi.org/10.1016/j.ica.2022.120946.
[37] C.J. Carrasco, F. Montilla, E. Álvarez, A. Galindo, M. Pérez-Aranda, E. Pajuelo, A. Alcudia, Homochiral imidazolium-based dicarboxylate silver(I) compounds: synthesis, characterisation and antimicrobial properties, Dalton Trans. 51 (2022) 5061–5071, https://doi.org/10.1039/D1DT04213K.
[38] C.J. Carrasco, F. Montilla, Á. Eleuterio, A. Alcudia, Antimicrobial properties of amino-acid-derived N-heterocyclic carbene silver complexes, Pharmaceutics 14 (2022) 748, https://doi.org/10.3390/pharmaceutics14040748.
[39] D. Tapu, D.A. Dixon, C. Roe, ^{13}C NMR spectroscopy of "Arduengo-type" carbenes and their derivatives, Chem. Rev. 109 (2009) 3385–3407, https://doi.org/10.1021/cr800521g.
[40] S. Weske, Y. Li, S. Wiegmann, M. John, H(C)Ag: a triple resonance NMR experiment for 109Ag detection in labile silver-carbene complexes, Magn. Reson. Chem. 53 (2015) 291–294, https://doi.org/10.1002/mrc.4196.
[41] U.J. Scheele, M. Georgiou, M. John, S. Dechert, F. Meyer, Combining pyrazolate and N-heterocyclic carbene coordination motifs: synthesis and characterization of a double-crowned silver complex, Organometallics 27 (2008) 5146–5151, https://doi.org/10.1021/om800487e.
[42] C.R. Groom, I.J. Bruno, M.P. Lightfoot, S.C. Ward, The Cambridge structural database, Acta Crystallogr, Sect. B Struct. Sci. Cryst. Eng. Mater. 72 (2016) 171–179, https://doi.org/10.1107/S2052520616003954.
[43] E.A. Baquero, G.F. Silbestri, P. Gómez-Sal, J.C. Flores, E. De Jesús, Sulfonated water-soluble N-heterocyclic carbene silver(I) complexes: behavior in aqueous medium and as NHC-transfer agents to platinum(II), Organometallics 32 (2013) 2814–2826, https://doi.org/10.1021/om400228s.

[44] L.R. Moore, S.M. Cooks, M.S. Anderson, H.J. Schanz, S.T. Griffin, R.D. Rogers, M. C. Kirk, K.H. Shaughnessy, Synthesis and characterization of water-soluble silver and palladium imidazol-2-ylidene complexes with noncoordinating anionic substituents, Organometallics 25 (2006) 5151–5158, https://doi.org/10.1021/om060552b.

[45] M. Marinelli, M. Pellei, C. Cimarelli, H.V.R. Dias, C. Marzano, F. Tisato, M. Porchia, V. Gandin, C. Santini, Novel multicharged silver(I)–NHC complexes derived from zwitterionic 1,3-symmetrically and 1,3-unsymmetrically substituted imidazoles and benzimidazoles: synthesis and cytotoxic properties, J. Organomet. Chem. 806 (2016) 45–53, https://doi.org/10.1016/j.jorganchem.2016.01.018.

[46] G. Papini, M. Pellei, G. Gioia Lobbia, A. Burini, C. Santini, Sulfonate- or carboxylate-functionalized N-heterocyclic bis-carbene ligands and related water soluble silver complexes, Dalton Trans. (2009) 6985–6990, https://doi.org/10.1039/b906994a.

[47] A. Almássy, C.E. Nagy, A.C. Bényei, F. Joó, Novel sulfonated N-heterocyclic carbene gold(I) complexes: homogeneous gold catalysis for the hydration of terminal alkynes in aqueous media, Organometallics 29 (2010) 2484–2490, https://doi.org/10.1021/om1001292.

[48] D. Nemcsok, K. Wichmann, G. Frenking, The significance of π interactions in group 11 complexes with N-heterocyclic carbenes, Organometallics 23 (2004) 3640–3646, https://doi.org/10.1021/om049802j.

[49] G. Lv, L. Guo, L. Qiu, H. Yang, T. Wang, H. Liu, J. Lin, Lipophilicity-dependent ruthenium N-heterocyclic carbene complexes as potential anticancer agents, Dalton Trans. 44 (2015) 7324–7331, https://doi.org/10.1039/c5dt00169b.

[50] O. Kühl, S. Millinghaus, P. Wehage, Functionalised, chiral imidazolium compounds from proteinogenic amino acids, Open Chem. 8 (2010) 1223–1226, https://doi.org/10.2478/s11532-010-0097-9.

[51] P. Boukamp, R.T. Petrussevska, D. Breitkreutz, J. Hornung, A. Markham, N. E. Fusenig, Normal keratinization in a spontaneously immortalized aneuploid human keratinocyte cell line, J. Cell Biol. 106 (1988) 761–771, https://doi.org/10.1083/jcb.106.3.761.

[52] A.D. Becke, Density-functional thermochemistry. III. The role of exact exchange, J. Chem. Phys. 98 (1993) 5648–5652, https://doi.org/10.1063/1.464913.

[53] C. Lee, W. Yang, R.G. Parr, Development of the Colle-Salvetti correlation-energy formula into a functional of the electron density, Phys. Rev. B 37 (1988) 785–789, https://doi.org/10.1103/PhysRevB.37.785.

[54] P.J. Hay, W.R. Wadt, Ab initio effective core potentials for molecular calculations. Potentials for K to au including the outermost core orbitale, J. Chem. Phys. 82 (1985), https://doi.org/10.1063/1.448975.

[55] Gaussian 09, Revision B.01, M. J. Frisch, G. W. Trucks, H. B. Schlegel, G. E. Scuseria, M. A. Robb, J. R. Cheeseman, G. Scalmani, V. Barone, G. A. Petersson, H. Nakatsuji, X. Li, M. Caricato, A. Marenich, J. Bloino, B. G. Janesko, R. Gomperts, B. Mennucci, H. P. Hratchian, J. V. Ortiz, A. F. Izmaylov, J. L. Sonnenberg, D. Williams-Young, F. Ding, F. Lipparini, F. Egidi, J. Goings, B. Peng, A. Petrone, T. Henderson, D. Ranasinghe, V. G. Zakrzewski, J. Gao, N. Rega, G. Zheng, W. Liang, M. Hada, M. Ehara, K. Toyota, R. Fukuda, J. Hasegawa, M. Ishida, T. Nakajima, Y. Honda, O. Kitao, H. Nakai, T. Vreven, K. Throssell, J. A. Montgomery, Jr., J. E. Peralta, F. Ogliaro, M. Bearpark, J. J. Heyd, E. Brothers, K. N. Kudin, V. N. Staroverov, T. Keith, R. Kobayashi, J. Normand, K. Raghavachari, A. Rendell, J. C. Burant, S. S. Iyengar, J. Tomasi, M. Cossi, J. M. Millam, M. Klene, C. Adamo, R. Cammi, J. W. Ochterski, R. L. Martin, K. Morokuma, O. Farkas, J. B. Foresman, D. J. Fox, Gaussian, Inc., Wallingford CT, 2016.

[56] Bruker, SAINT+, SAINT+, Bruker AXS Inc, Madison, Wisconsin, USA, 2007.

[57] G.M. Sheldrick, SADABS, Programs for Scaling and Absorption Correction of Area Detector Data, SADABS, Programs Scaling Absorpt. Correct. Area Detect. Data, University of Göttingen, Göttingen, Germany, 1997.

[58] M.C. Burla, M. Camalli, B. Carrozzini, G.L. Cascarano, C. Giacovazzo, G. Polidori, R. Spagna, SIR2002 : the program, J. Appl. Crystallogr. 36 (2003) 1103, https://doi.org/10.1107/S0021889803012585.

[59] G.M. Sheldrick, A short history of SHELX, Acta Crystallogr. Sect. A Found. Crystallogr. 64 (2008) 112–122, https://doi.org/10.1107/S0108767307043930.

[60] P. Van Der Sluis, A.L. Spek, BYPASS: an effective method for the refinement of crystal structures containing disordered solvent regions, Acta Crystallogr. Sect. A. 46 (1990) 194–201, https://doi.org/10.1107/S0108767389011189.